African Journal of Pharmaceutical Research and Development
Available online at https://ajopred.com
Vol. 16 No.1; pp. 14-25 (2024)

Original Research Article

DEMETHOXYLATED CURCUMINOIDS AS ANTIDIABETIC COMPLICATION DRUG LEADS – *IN SILICO* STUDIES

OLUSEGUN SAMSON AJALA[1,*], DOLAPO OMOLADE INNOCENT-UGWU[1], PEACE UDODIRI OKECHUKWU[1], OLAYINKA HANNAH DADA[1]

1. Department of Pharmaceutical Chemistry, Faculty of Pharmacy, University of Lagos, CMUL Campus Idiaraba, P.M.B. 12003, Surulere, Lagos.

ABSTRACT

Curcuma longa is used traditionally in the treatment of diabetes and diabetic complications. Aldose Reductase (ALR2) inhibition is a plausible therapeutic strategy against diabetic complications. This work was aimed at evaluating *Curcuma longa* phytochemicals, *in silico*, for their ALR2 inhibitory potentials. Thirty-nine (39) phytoconstituents of *Curcuma longa* were subjected to a succession of *in silico* screenings comprising molecular docking, drug-likeness and safety profiling to identify ALR2 inhibitor leads, validating their binding interactions with molecular dynamics simulations at 50 ns simulation time. The *in silico* evaluations afforded two demethoxylated curcuminoids, bisdemethoxycurcumin and demethoxycurcumin, as potential ALR2 inhibitor leads forming stable ALR2 complexes, their relative potencies correlating to their degrees of demethoxylation. The two curcuminoids are herein recommended as leads for the discovery of ALR2 inhibitory antidiabetic complication drug leads.

ARTICLE INFO

Received 16 October, 2023
Accepted 14 January, 2024
Published 30 January, 2024

KEYWORDS

In silico drug discovery,
Aldose reductase inhibition,
Curcuma longa,
Curcuminoids,
Diabetic complication

INTRODUCTION

Diabetes mellitus is a metabolic disease characterized by elevated blood glucose level (or hyperglycemia) originating from impairment of insulin secretion and/or action [1]. Regardless of etiology, prolonged or unchecked hyperglycemia results into oxidative and at times, osmotic, stresses leading to devastating tissue damages summarily described as diabetic complications, and to which diabetes owes its high morbidity and mortality [2]. Commonly reported of such complications include retinopathy, neuropathy, nephropathy and various cardiomyopathies, e.g., stroke [2, 3].

Hyperglycemia-induced oxidative stress, in particular, plays a pivotal role in the pathogenesis of diabetic complications, as supported by reports of increase in levels of oxidised cellular macromolecules in virtually all cases of diabetic complications [4, 5]. This is probably rooted in the multiple ways via which increased blood glucose level may induce oxidative stress. These include direct glucose involvement in the impairment of cellular antioxidant defence by anti-oxidant enzyme glycation as seen in Superoxide Dismutase glycation [6, 7], and in the generation of Reactive Oxygen Species (ROS) via glucose

***Corresponding author:** olajala@unilag.edu.ng; +234-803 562 2151

https://doi.org/10.59493/ajopred/2024.1.2 ISSN: 0794-800X (print); 1596-2431 (online)

auto-oxidation, mitochondrial electron transport distruption, and non-enzymatic glycation processes leading to Advanced Glycation End-products (AGEs) formation [8, 9]. Yet another hyperglycemia-induced oxidative stress mechanism is the activation of the polyol pathway of glucose metabolism. It is an indirect mechanism as it is devoid of direct glucose action which either generates ROS or depletes cells of defence antioxidant enzymes as seen in the afore-listed mechanisms. It is an alternate glucose metabolism pathway that is rather inconsequential in normoglycemia as it is normally responsible for the bioconversion of only about 2 % of total blood glucose [10]. In protracted hyperglycemia, however, it becomes activated and responsible for the bioconversion of up to 30% of the already elevated blood glucose, leading to accumulation of sorbitol, the formation of which is accompanied with oxidative stress via three different mechanisms involving direct glycation and ROS formation via coupled reactions ensuing from cofactor dependence of the pathway's two enzymes, aldose reductase (ALR2) and sorbitol dehydrogenase (SDH) [11].

The first mechanism of oxidative stress induction by polyol pathway activation is mediated by its first step, the rate-limiting ALR2-dependent conversion of glucose to sorbitol. This step occurs at the expense of reduced Nicotinamide Adenine Dinucleotice Phosphate (NADPH), causing a depletion of the cellular antioxidant Glutathione (GSH), the synthesis of which requires NADPH [12]. Another oxidative stress mechanism of polyol pathway activation is borne out of the activity of the second enzyme of the pathway, SDH, in the conversion of sorbitol to fructose. This conversion requires the oxidised Nicotinamide Adenine Dinucleotide (NAD^+) as cofactor, leading to cellular accumulation of the reduced cofactor (NADH) which is the substrate of NADH oxidase, involved in the synthesis a number of ROS [13]. The third oxidative stress induction mechanism of polyol pathway activation is owed to the chemical nature of its fructose end product and possible derivatives (fructose-3-phosphate and 3-deoxyglucosone), which are naturally stronger glycating agents than glucose, leading to formation of AGEs and consequent ROS [14, 15].

ALR2, being a pathway's rate-limiting enzyme would ordinarily offer itself as a plausible drug discovery target. This probably explains why ALR2 has been the target focus of many antidiabetic complication drug discovery projects [16, 17]. Notwithstanding, there is yet a paucity of such agents in antidiabetic drug therapy [18, 19]. The paucity of clinical antidiabetic complication ALR2 inhibitors could be attributed to reasons bordering on safety and selectivity of candidates [20]. This in turn may not be unconnected to the fact that ALR2 is closely related to another aldo-ketoreductase, aldehyde reductase (ALR1) [21], which is crucial to the metabolic clearance of reactive aldehydic xenobiotics and metabolites of many biochemical processes, the systemic accumulation of which could be devastating physiologically [22, 23]. There remains therefore a high need for the discovery of new ALR2 inhibitors that would be safe and selective enough to be deployed clinically as routine medications in antidiabetic drug management to prevent or treat diabetic complications.

Exploring folkloric uses of medicinal plants remains a viable drug lead discovery approach [24, 25]. Looking for antidiabetic complication drug leads from medicinal plants with folkloric antidiabetic/antidiabetic complication claims should therefore be a right step towards discovering antidiabetic complication drug leads [26, 27]. Such is *Curcuma longa,* a Rhizomatous herbaceous perennial in the Zingiberaceae plant family. It is a food and medicinal plant noted for its folkloric antidiabetic/antidiabetic complication claims. Its chemistry is dominated by the presence of plain and conjugated diarylheptanoids generally referred to as curcuminoids and to which Curcuma longa is believed to largely owe its spicy and therapeutic properties despite reports of presence of other phytochemical groups, including alkaloids, coumarins and flavonoids [28, 29].

In this investigation, we aimed at a possible discovery of antidiabetic complication drug leads from both cucuminoid and non-curcuminoid phytoconstituents of *Curcuma longa,* using in silico techniques.

MATERIALS AND METHODS

Materials and Softwares

All *in silico* protocols were carried out on an HP ProBook equipped with intel Core i5, 500GB Hard Disk, 8 GB RAM; Protein preparations were done using UCSF Chimera 1.14 [30]; 2D and 3D ligand-macromolecule complex interactions were visualized using BIOVIA Discovery studio visualizer 2021 [31]; multiple ligands docking was carried out with PyRx [32] molecular docking software equipped with AutoDock Vina and Open Babel plugins; SwissADME [33] and Protox II [34] webservers were used for drug-likeness and toxicity profilings respectively; molecular dynamics simulations were performed using the University of Arkansas for Medical Sciences (UAMS) simlab WebGro [35] webserver; other webservers visited in the course of this study included: RCSB Protein Databank (PDB) [36], Pubchem [37], PRODRG [38], CASTp [39] and Uniprot [40].

Protein Preparation

An X-ray crystal model of a ternary (ALR2; PDBID 1AH3; 2.30 Å), was uploaded into Chimera 1.14 workspace by direct fetch. All non-standard residues including tolrestat, the cocrystallized inhibitor, the coenzyme NADPH and water molecules were removed. Hydrogen atoms and amber charges were added and the structure subsequently minimized using 200 steepest descent and 10 conjugate gradient steps energy minimization algorithm of the software. The ensuing prepared protein structure was saved for subsequent uses.

Docking Protocol Validation

Tolrestat structure data was built into the *Curcuma longa* phytoconstituent library file and docked alongside the phytoconstituents into the mapped site in the macromolecule. The coordinates of the native and those of the lowest-energy pose of the docked tolrestat were subsequently superimposed

and RMSD calculated, using BIOVIA Discovery Studio visualizer.

Curcuma longa Ligands Preparation

Thirty-nine (39) compounds of *Curcuma longa* identified from literature [28, 29] were retrieved from Pubchem database as structure data files and built into a one-file library. The library file was uploaded into the Open Babel workspace of PyRx for energy minimization and subsequent conversion into pdbqt (or autodock-compliant) ligands.

Multiple Ligands Docking

Prepared pig ALR2 (PDBID 1AH3) was uploaded into the PyRx docking workspace and made macromolecule. The *Curcuma longa* phytoconstituents library file was imported into the docking workspace and the 39 compounds therein (comprising curcuminoids, coumarins and flavonoids) selected as ligands before the autodock vina algorithm was run, using the three-dimensional coordinates of the native tolrestat molecule as guide for docking-site mapping, translating to the following grid-box coordinates (in Angstroms): center_x = 67.1699493018; center_y = 40.4447862549; center_z = 90.9558925756; size x = 17.3125093612; size_y = 14.9676312165.

Drug-likeness and Toxicity Profilings

Fifteen topmost of the phytoconstituents, having their docking scores comparable to that of tolrestat, were selected as hits and screened against the five (i.e., Lipinski, Verber, Ghose, Muegge and Egan) drug-likeness filters in the SwissADME webserver, setting violation of none of the stipulations of each of the filters as criterion for drug-likeness selection. The ensuing seven, based on this criterion, were further screened through the toxicity prediction algorithm of Protox II webserver to identify leads on the basis of high (≥ 1500 mg/Kg) LD50 and absence of organ and toxicity endpoint tendencies of carcinogenicity, cytotoxicity, hepatotoxicity, immunotoxicity and mutagenicity. Canonical SMILES [41] were used as the main inputs of both screenings.

Molecular Dynamics Simulations

The binding interactions of the identified leads were validated by carrying out molecular dynamics simulation studies on their ALR2 complexes using Webgro, the University of Arkansas for Medical Sciences (UAMS) webserver for molecular dynamics simulation. Independent variable parameters were set as follows: Box type was triclinic with SPC water model; GROMOS9643a1 was selected as force field; equilibrium temperature was 300 K, while simulation time was set at 50 ns. Ligand - macromolecule complexes were prepared as pdb files with BIOVIA Discovery Studio; Ligand topology files were prepared with PRODRG webserver, using coordinates extracted from the text formats of the complexes.

RESULTS

Docking Validation

The coordinates of the docked tolrestat in its best-pose conformation superimposed well on those of its native counterpart with a calculated 1.46 Å RMSD.

Molecular Docking

Tolrestat was re-docked with a binding energy of - 8.8 Kcal/mol. The thirty-nine *Curcuma longa* phytoconstituents docked with binding energies ranging from - 9.6 Kcal/mol to - 5.5 Kcal/mol. Fifteen (15) of them (comprising 11 curcuminonid-skeleton comtaining compounds, 3 flavonoids and one sesquiterpenoid) showed comparable binding energies (-9.6 Kcal/mol to - 8.3 Kcal/mol) to the - 8.8 Kcal/mol of the native ligand and thus selected as hits, the curcuminoid bisdemethoxycurcumin showing the best (-9.6 Kcal/mol) docking score. Table 1 shows the details of the ALR2 binding energies of tolrestat and the selected hits.

Drug-likeness and Toxicity Potentials Screenings

Seven of the fifteen hits (comprising four curcuminoids and three flavonoids) fulfilled the set criterion for drug-likeness, violating none of the stipulations of each of the five drug-likeness filters of SwissADME (Table 2). They demonstrated LD_{50} values ranging from 1500 to 3919 mg/Kg. The three flavonoids showed tendencies of cytotoxicity while curcurmin and cyclocurcumin showed tendencies of immunotoxicity. Bisdemethoxycurcumin and demethoxycurcumin showed no tendency of inducing any of the toxicity parameters tested. Table 3 shows the predicted toxicities of the aforementioned six compounds.

Molecular Dynamics

The ALR2 complexes of bisdemethoxycurcumin (BDMC) and demethoxycurcumin (DMC) converge around 2 ns and 15ns respectively. The two complexes however stayed largely within a deviation of 2.5 Å from their respective initial structures in the course of 50 ns simulation time (Fig. 1). ALR2 in the ALR2-BDMC complex showed significant fluctuations in the equilibrium positions of the residues around 130 and 220 positions while residues around positions 70, 130, 220 and 270 suffered significant fluctuations in the DMC complex. However, the overall degree of fluctuations for BDMC and DMC in their respective complexes were approx. 4.5 Å and 3.5 Å respectively. These fluctuations are as depicted in the RMSF plots in Fig. 2.

Each curcuminoid ligand experienced an overall approx. 5 Å from its initial conformation, the constancy of this deviation more largely maintained in DMC over the 50 ns simulation time than in BDMC (Fig. 3). And despite these immense curcuminoid conformational variations, the radii of gyration of complexes were largely maintained at around 19 Å (Fig. 4).

Table 1: Tolrestat and 15 Curcuma longa phytoconstituents arranged in order of decreasing docking score (or binding affinity) in Kcal/mol

S/N	Name	Binding energy (Kcal/mol)
1	Tolrestat	-8.8
2	Bisdemethoxycurcumin	-9.6
3	Terpecurcumin R	-9.3
4	Terpecurcumin O	-9.2
5	Demethoxycurcumin	-9.1
6	Terpecurcumin J	-9.1
7	Curcumin	-9.0
8	Curcumin glucuronide	-8.9
9	Cyclocurcumin	-8.9
10	Terpecurcumin U	-8.9
11	Genistein	-8.8
12	Tetrahydrocurcumin	-8.7
13	Apigenin	-8.5
14	Kaempferol	-8.4
15	Terpecurcumin N	-8.3
16	Tumerone	-8.3

Table 2: Violation patterns of Lipinski, Verber, Ghose, Muegge and Egan drug-likeness filters by fifteen ALR2-inhibiting hits from *Curcuma longa*

S/N	Compound	Lipinski	Ghose	Veber	Egan	Muegge	Bioavailability Score
1	Bisdemethoxycurcumin*	0	0	0	0	0	0.55
2	Terpecurcumin R	1	4	1	1	1	0.55
3	Terpecurcumin O	1	4	1	1	1	0.56
4	Demethoxycurcumin	0	0	0	0	0	0.55
5	Terpecurcumin J	1	4	0	1	1	0.56
6	Curcumin*	0	0	0	0	0	0.55
7	Curcumin glucuronide	2	2	2	1	2	0.11
8	Cyclocurcumin*	0	0	0	0	0	0.56
9	Terpecurcumin U	1	4	1	1	1	0.56
10	Genistein*	0	0	0	0	0	0.55
11	Tetrahydrocurcumin	1	0	1	1	2	0.11
12	Apigenin*	0	0	0	0	0	0.55
13	Kaempferol*	0	0	0	0	0	0.55
14	Terpecurcumin N	1	4	1	1	1	0.56
15	Tumerone	0	0	0	0	1	0.55

**violated none of the stipulations of each of the five filters*

Table 3: Predicted toxicity profiles of six drug-like ALR2-inhibiting hits

S/N	Compound	LD50 (mg/Kg)	Organ toxicity/Toxicity endpoints				
			Hepato Toxicity	Carcino Genicity	Immuno toxicity	Cyto toxicity	Muta genicity
1	BDMC	2560	-	-	-	-	-
2	DMC	2000	-	-	-	-	-
3	Curcumin	1500	-	-	Active	-	-
4	Cyclocurcumin	1500	-	-	Active	-	-
5	Genistein	2500	-	-	-	Active	-
6	Apgenin	2500	-	-	-	Active	-
7	Kaempferol	3919	-	-	-	Active	-

- = Not active
BDMC = Bisdemethoxycurcumin
DMC = Demethoxycurcumin

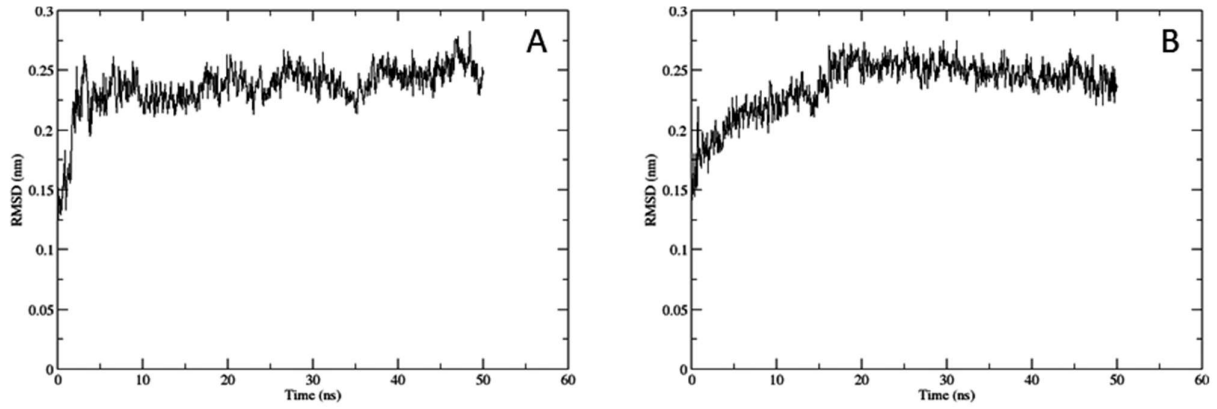

Fig. 1: RMSD plots of ALR2 complexes with A – bisdemethoxycurcumin (BDMC) and B – demethoxycurcumin (DMC) in a 50 ns molecular dynamics simulation.

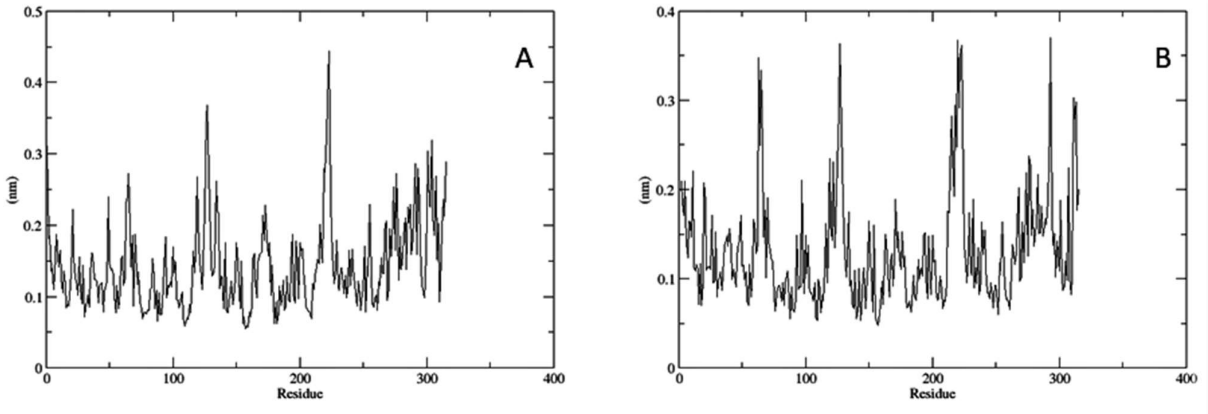

Fig. 2: RMSF plots of ALR2 complexes with A – bisdemethoxycurcumin (BDMC) and B – demethoxycurcumin (DMC) after 50 ns molecular dynamics simulations

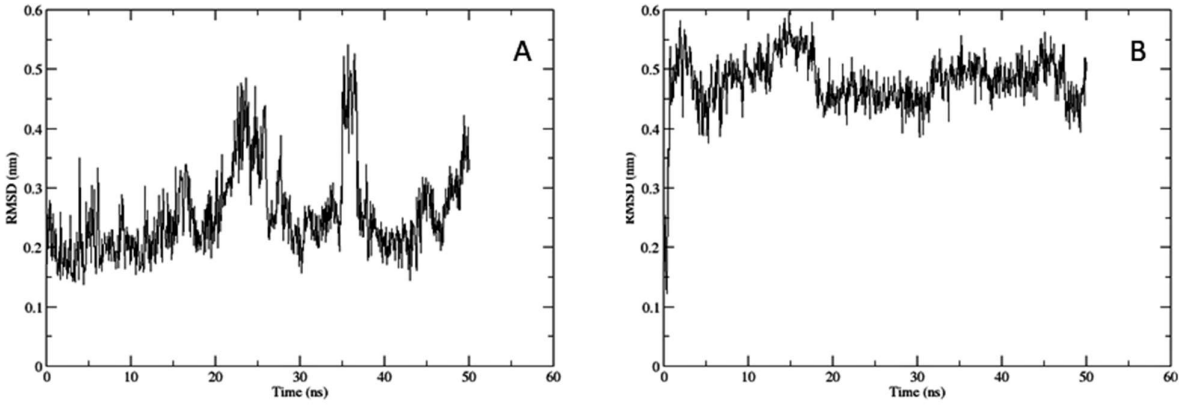

Fig.3: RMSD plots of A - bisdemethoxycurcumin (BDMC) and B- demethoxycurcumin (DMC) in the ALR2 binding pocket

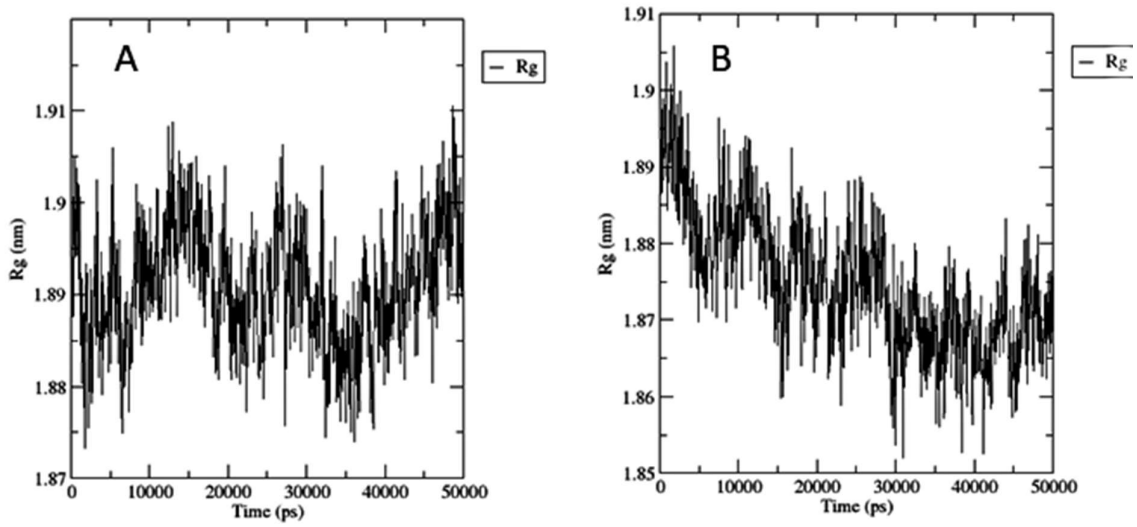

Fig. 4: Radius of gyration (RoG) of A – bisdemethoxycurcumin (BDMC) and B- demethoxycurcumin (DM

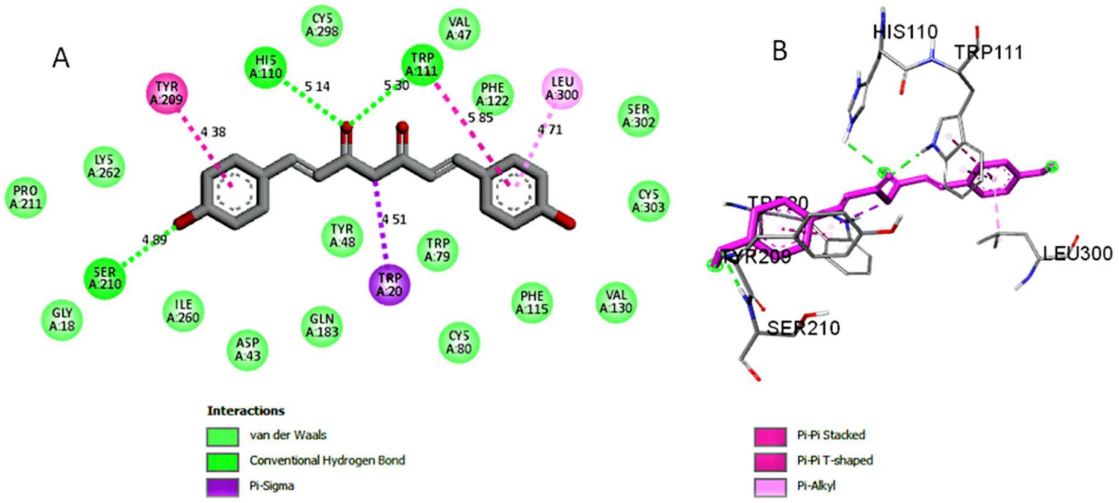

Fig. 5: A – 2D and B – 3D simulations of the binding interactions of bi of bisdemethoxycurcumin (BDMC) with amino residues at ALR2 active site

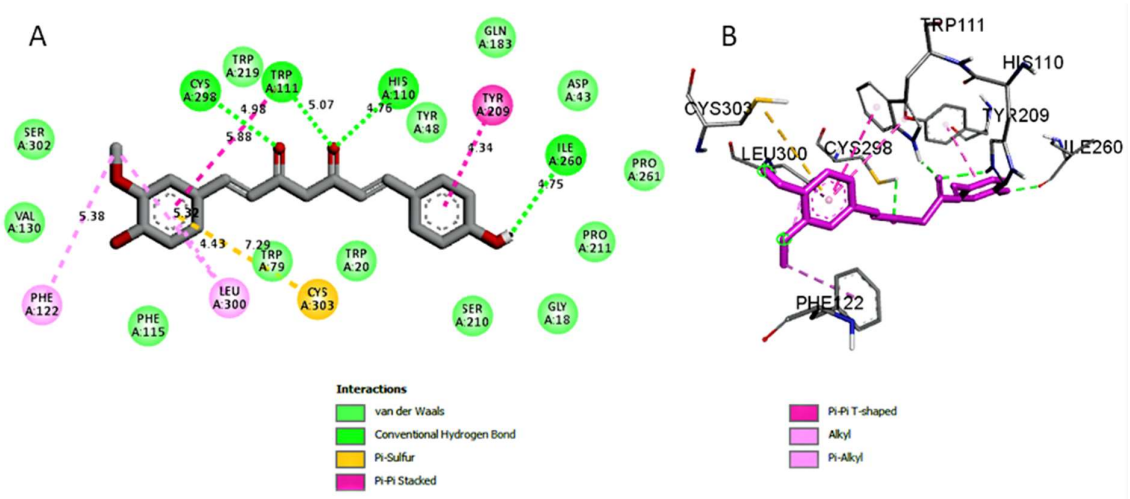

Fig. 6: A – 2D and B – 3D simulations of the binding interactions of bi of demethoxycurcumin (DMC) with amino residues at ALR2 active site

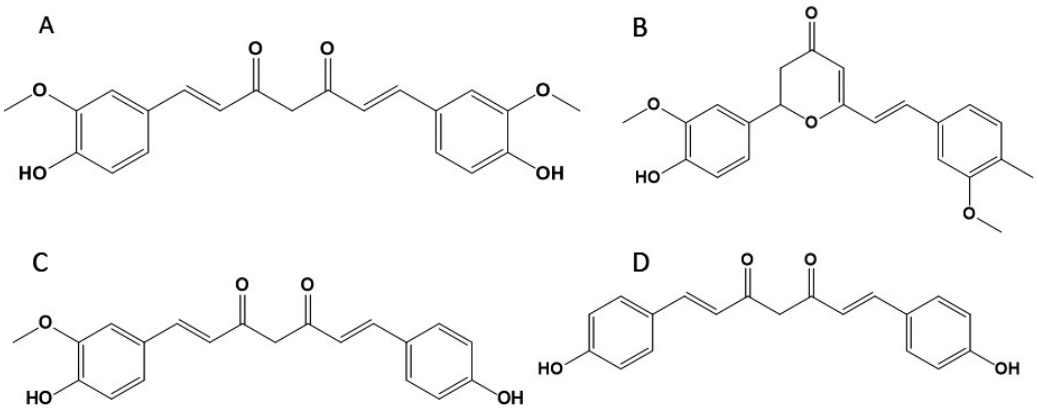

Fig. 7: 2D structures of : A- curcumin; B- cyclocurcumin; C- demethoxycurcumin (DMC) and D – bisdemethoxycurcumin (BDMC)

Binding Interactions of Bisdemethoxycurcumin and Demethoxycurcumin at ALR2 Active Site

BDMC was held in place in the binding pocket by three conventional hydrogen bonds with the residues HIS110, TRP111, SER210 in addition to other supramolecular interactions including pi-pi, pi-sigma and van der Waals forces (Fig. 5). The hydrogen bonds with HIS110 and TRP110 were preserved in DMC interactions. Additional hydrogen bonds (with ILE260 and CYS298 residues) were however notable addition to other supramolecular pi-pi stacked, pi-pi T-shaped and van der Waals forces (Fig. 6).

DISCUSSION

Ever since the discovery of the antidiabetic-complication therapeutic potentials of ALR2 inhibition, concerted efforts have poured ceaselessly into the discovery of ALR2 inhibitors. Despite over four decades of search, however, existing inhibitors have failed to obtain globally persuasive clinical success as they are yet to convincingly prove the arrest of the cellular maladies of diabetic complications [42]. One major roadblock to the discovery of clinical ALR2 inhibitors with the desired effectiveness is the high toxicity tendency of potential inhibitors predicated largely on their unwanted inhibition of a closely related aldo-ketoreductase, aldehyde reductase (ALR1) [43]. Deployment of *in silico* techniques on one hand, therefore, would not only fast-track discovery, but would actually minimize

or eliminate losses accruable to failing late in the discovery cascade [44]. On the other hand, the use of natural product as leads or initial templates would take advantage of nature's unique associated structural novelty and/or functional intricacies necessary for the achievement of the required selectivity [45, 46]. This investigation attempted harmonizing these merits by subjecting the phytoconstituents of *Curcuma longa* to a battery of *in silico* evaluations, leading to the identification of two curcuminoids, bisdemethoxycurcumin and demethoxycurcumin, as ALR2 inhibitory antidiabetic-complication drug leads.

The PDB ALR2 model (1AH3) used was adjudged suitable for the docking experiment on account of its good 2.30 Å resolution and for being an inhibitor conformation model of the holo form of the enzyme [47]. The 1.46 Å root mean square deviation (RMSD) between the docked and native poses of the co-crystalized ligand, tolrestat, validated the docking protocol as reliable [48]. Docking 39 phytoconstituents of *Curcuma longa* (including flavonoids, coumarins, sesterpenes, curcuminoids and curcuminoid conjugates, etc.) and arranging the ensuing docking scores in increasing order of binding energies led to the identification of fifteen compounds with docking scores comparable to the -8.8 Kcal/mol binding energy of the re-docked co-crystalized inhibitor, tolrestat, and hence selected as hits [49, 50], comprising three natural curcuminoids (curcumin, demethoxycurcumin and bisdemethoxycurcumin); one cyclic curcuminoid derivative (cyclocurcumin); five curcuminoid sesquiterpene conjugates (terpecurcumins J, O, N, R, U); one glucuronide conjugate (curcumin glucuronide); one sesquiterpene (tumerone) and three flavonoids (genistein, apigenin and kaempferol) (Table 1). As ALR2 inhibitor hits, they all have very great propensities of interacting with ALR2 in an inhibitory manner. However, given that most drugs that fail late in the drug discovery process fail on pharmacokinetics and toxicity accounts, it is now considered that leads entering the design stage of drug discovery should have optimum pharmacokinetics/drug likeness and safety profiles [51-53]. Hence, the Pharmacokinetics/drug-likeness and toxicity profiling segments of the *in silico* screenings.

The SwissADME webserver has, *inter alia*, algorithms for five different drug-likeness filters namely Lipinski, Verber, Ghose, Muegge and Egan filters [54]. Each of these filters has a number of rules and a pre-set condition as to the number of violations permissible to qualify as drug-like [54]. Because of the variations in the physicochemical basis of the filters and in the number of violations permissible, we set non-violation of any stipulation of each of the filters as condition for drug-likeness selection. Only seven of the fifteen hits subjected to the drug-likeness screening fulfilled this rather strict criterion (Table 2). The seven compounds comprised four curcuminoids and three flavonoids. The curcuminoid components were made up of the three natural curcuminonids (curcumin, demethoxycurcumin and bisdemethoxycurcumin) and a cyclic derivative of curcumin (cyclocurcumin) while the flavonoid components are genistein, apigenin and kaempferol. It is worthy of note that all the curcuminoid conjugates (comprising curcumin glucuronide and the five sesquiterpene conjugates, terpecurcumins J, O N, R and U) did not make the drug-like compounds list. Their huge molecular weights contributed in no small ways to this failure as each of them has a molecular weight > 500 g/mol, a violation of one of the four stipulations of the Lipinski's filter [53]. The failure of tumerone, a rather small molecule of optimum molecular weight (MW 218.33 g/mol) was due to the strictness of the set criterion of not violating any of the stipulations of each of the five filters. Tumerone violated only one of only the Muegge filter's stipulations [55].

The last port of call in the ALR2 inhibitor leads screen was toxicity profiling. This was imperative because in addition to toxicity contributing immensely to failing at clinical trial stages of the drug discovery process in general, it would much more to ALR2 inhibitors discovery in particular because of the need for potential inhibitors to bind selectively to ALR2, sparing the closely related aldo-ketoreductase aldehyde reductase (ALR1). Final lead selection was done from the drug-like hits list based on having a minimum of 1500 mg/kg LD_{50} and lack of tendency to induce organ toxicity and toxicity endpoints parameterized as hepatotoxicity, cytotoxicity, immunotoxicity, carcinogenicity and mutagenicity. All the seven candidates of this toxicity screening demonstrated an LD_{50} of 1500 mg/kg or greater, showing that whatever toxicity tendency any of them may show is not likely to occur within a human tolerable dose range. Notwithstanding, weeding off candidates with traces of sign of toxicity would be of utmost interest in a discovery program as ALR2 inhibitors discovery wherein toxicity of prospective inhibitors has been the albatross of decades of concerted discovery efforts [56]. Hence, the key role that manifestation of organ toxicity and toxicity endpoints played in the final lead selection.

The three flavonoids, kaempferol, apigenin, and genistein, showed cytotoxicity tendencies and therefore were not selected. This is attributable to their compact and flat structures which makes them amenable to intercalation of DNA double helices and hence possibly interfere with cell division [57]. In the same vein, curcumin and its cyclic derivative cyclocurcumin showed immunotoxicity tendencies, leaving bisdemethoxycurcumin (BDMC) and demethoxycurcumin (DMC) as the only two compounds showing no toxicity tendencies at all. Unlike the flavonoids, structural rationalization of the toxicity tendencies of curcumin and cyclocurcumin is not facile. Nevertheless, the simple but rather striking structural difference between curcumin/ cyclocurcumin pair on one hand and demethoxycurcumin/bisdemethoxycurcumin pair on another, can be speculated upon to account for their different potential toxicities as follows: The basic curcuminoid skeleton is essentially made up of a fully conjugated C7 hydrocarbon chain flanked by two oxygenated aromatic rings. While in curcumin and cyclocurcumin, aromatic oxygenation is by methoxy and hydroxyl substitutions, it is short of one and the two methoxy groups in DMC and BDMC respectively (Fig. 7).

Aromatic methoxylation could have profound electronic and steric consequences on the chemical and biochemical properties of a molecule [58]. The lack of one and two aromatic methoxy groups respectively in DMC and BDMC, compared to

curcumin, therefore, is enough to influence their macromolecular interactions and, by extension, their toxicity profiles as observed. This also, in a way, explains the minor variations seen in the ALR2 interaction patterns of these demethoxylated curcuminoids selected as ALR2 inhibitor leads. Apart from induced fit docking (IFD) which incorporates algorithms to account for momentary atomic displacements during binding, molecular docking algorithms in general do not take the dynamic nature and environments of biological systems into consideration [59]. Molecular docking experiments, which incidentally forms the foundation of structure-based *in silico* evaluations, could therefore give spurious or misleading results and would often require further *in silico* validation before proceeding to *in vitro* and *in vivo* confirmations. In this investigation, the binding interaction information obtained from the molecular docking experiments with the selected leads, DMC and BDMC, were validated in molecular dynamics simulation experiments. Analysis of the MD results indicated that the two leads form stable ALR2 complexes, with BDMC demonstrating more stable characteristic features than DMC. The convergence of the instantaneous and initial complex structures occurred much faster with BDMC than DMC (2 s and 15 s respectively). However, the maintenance of the deviation of each complex from the initial structure below 3 Å (around 2.5 Å) is a strong indication of stability of the two complexes in the rather dynamic physiological environment [60]. Analysis of the ligand RMSD plots in Figure 3 showed that there is a great deal of deviation (5 Å) of each of DMC and BDMC in the binding pocket of the enzyme, though DMC appeared to enjoy a better constancy of this deviation over the simulation time period. And though the Radii of Gyration (RoGs) of the protein in the two complexes were maintained at the modest values around 19 Å, more or less corroborating stability [61], RMSF plots showed that fluctuations of residues about their equilibrium positions in the course of the simulations affected more residues in DMC than BDMC. These marginal differences observed in the dynamics of the two demethoxylated curcuminoids can also be attributed to their different degree of demethoxylation compared to the parent curcuminoid skeleton.

CONCLUSION

Combining the rational nature of in silico drug discovery techniques with the structural novelty of natural products, Aldose Reductase (ALR2) inhibitor leads were sought from *Curcuma longa* phytoconstituents. Two curcuminoids, bisdemethoxycurcumin and demethoxycurcumin, deprived respectively of one and two aromatic methoxy groups (compared to the basic curcuminoid skeleton) were identified as leads. This work has in a way provided molecular rationales for the antidiabetic complication claims in the traditional use of *Curcuma longa*. It has also uncovered two natural product leads that could be further explored via *in vivo, in vitro* and molecular modification studies towards the discovery of new ALR2 inhibitory antidiabetic complication agents.

CONFLICT OF INTEREST

Authors declare no conflict of interest.

REFERENCES

1. Adeghate E, Schattner P, Dunn E. An update on the etiology and epidemiology of diabetes mellitus. Annals of New York Academy of Science, 1084(1), 2006:1-29.
2. Brownlee M. Biochemistry and molecular cell biology of diabetic complications. Nature, 414(6865), 2001:813-820.
3. Altan VM. The pharmacology of diabetic complications. Current Medicinal Chemistry, 10(15), 2003:1317-27.
4. Wei W, Liu Q, Tan Y, Liu L, Li X, Cai L. Oxidative stress, diabetes, and diabetic complications. Hemoglobin, 33(5), 2009:370-377.
5. Iacobini C, Vitale M, Pesce C, Pugliese G, Menini S. Diabetic complications and oxidative stress: A 20-year voyage back in time and back to the future. Antioxidants, 10(5), 2021:727-750.
6. Kawamura N, Ookawara T, Suzuki, K, Konishi, Mino M, Taniguchi, N. Increased glycated Cu, Zn-superoxide dismutase levels in erythrocytes of patients with insulin-dependent diabetes mellitus. Journal of Clinical Endocrinology and Metabolism, 74, 1992:1352–1354.
7. Morgan PE, Dean RT, Davies MJ. Inactivation of cellular enzymes by carbonyls and protein-bound glycation/glycoxidation products. Archives of Biochemistry and Biophysics, 403, 2002:259–269.
8. Kennedy AL, Lyons TJ. Glycation, oxidation, and lipoxidation in the development of diabetic complications. Metabolism: Clinical and Experimental, 46, 1997:14–21.
9. Yim MB, Yim HS, Lee C, Kang SO, Chock PB. Protein glycation: creation of catalytic sites for free radical generation. Annals of New York Academy of Sciences, 928, 2001:48–53.
10. Chung SS, Ho EC, Lam KS, Chung SK. Contribution of polyol pathway to diabetes-induced oxidative stress. Journal of the American Society of Nephrology, 14(suppl 3), 2003: S233-236.
11. Giacco F, Brownlee M. Oxidative stress and diabetic complications. Circulation Research, 107(9), 2010:1058-1070.
12. Cheng HM, Gonzalez RG. The effect of high glucose and oxidative stress on lens metabolism, aldose reductase and senile cataractogenesis. Metabolism: Clinical and Experimental, 35, 1986:10-14.
13. Morre DM, Lenaz G, Morre DJ. Surface oxidase and oxidative stress propagation in aging. Journal of Experimental Biology, 203, 2000:1513-1521.
14. Hamada Y, Araki N, Koh N, Nakamura J, Horiuchi S, Hotta N. Rapid formation of advanced glycation endproducts by intermediate metabolites of glycolytic pathway and polyol pathway. Biochemical and

Biophysical Research Communications, 228, 1996:539-543.
15. Hamada Y, Araki N, Horiuchi S, Hotta N. Role of polyol pathway in non-enzymatic glycation. Nephrology, Dialysis, Transplantation, 11(Suppl. 5), 1996b:95–98.
16. Miyamoto S. Recent advances in aldose reductase inhibitors: potential agents for the treatment of diabetic complications. Expert Opinion on Therapeutic Patents, 12(5), 2002:621-31.
17. El-Kabbani O, Ruiz F, Darmanin C, Chung RP. Aldose reductase structures: implications for mechanism and inhibition. Cellular and Molecular Life Sciences, 61, 2004:750-62.
18. Oka M, Kato N. Aldose reductase inhibitors. Journal of Enzyme Inhibition and Medicinal Chemistry, 16(6), 2001:465-473.
19. Pfeifer MA, Schumer MP, Gelber DA. Aldose reductase inhibitors: the end of an era or the need for different trial designs? Diabetes, 46(Supplement 2), 1997:S82-9.
20. Quattrini L, La Motta C. Aldose reductase inhibitors: 2013-present. Expert opinion on Therapeutic Patents, 29(3), 2019:199-213.
21. Bohren KM, Bullock B, Wermuth B, Gabbay KH. The aldo-keto reductase superfamily: cDNAs and deduced amino acid sequences of human aldehyde and aldose reductases. Journal of Biological Chemistry, 264(16), 1989:9547-9551.
22. Sato S, Kador PF. Inhibition of aldehyde reductase by aldose reductase inhibitors. Biochemical Pharmacology, 40(5), 1990:1033-1042.
23. Takahashi M, Miyata S, Fujii J, Inai Y, Ueyama S, Araki M, Soga T, Fujinawa R, Nishitani C, Ariki S, Shimizu T. In vivo role of aldehyde reductase. Biochemica et Biophysica Acta, 1820(11), 2012:1787-1796.
24. Gao H, Li G, Lou HX. Structural diversity and biological activities of novel secondary metabolites from endophytes. Molecules, 23(3), 2018:646.
25. Chopra B, Dhingra AK. Natural products: A lead for drug discovery and development. Phytotherapy Research, *35*(9), 2021: 4660-4702.
26. Karłowicz-Bodalska K, Han ST, Freier J, Smoleński M, Bodalska A. Curcuma longa as medicinal herb in the treatment of diabetic complications. Acta Poloniae Pharmaceutica-Drug Research, 74(2), 2017:605-610.
27. Silva PA, Arawwawala LD, Kumari MW, Galappatthy P. Effect of Curcuma longa L. and curcumin on diabetes and it's complications: A review. Journal of Ayurvedic and Herbal Medicine, 7(2), 2021:109-118.
28. Verma RK, Kumari P, Maurya RK, Kumar V, Verma RB, Singh RK. Medicinal properties of turmeric (Curcuma longa L.): A review. International Journal of Chemical Studies. 6(4), 2018:1354-7.
29. Chanda S, Ramachandra TV. Phytochemical and pharmacological importance of turmeric (Curcuma longa): A review. Research & Reviews: A Journal of Pharmacology, 9(1) 2019:16-23.
30. Pettersen EF, Goddard TD, Huang CC, Couch GS, Greenblatt DM, Meng EC, Ferrin TE. UCSF Chimera - A Visualization System for Exploratory Research and Analysis. Journal of Computational Chemistry, 25, 2004:1605-1612.
31. BIOVIA, Dassault Systèmes, BIOVIA Workbook, 2020.
32. Dallakyan S, Olson AJ. Small-Molecule Library Screening by Docking with PyRx. In: Hempel, J., Williams, C., Hong, C. (eds) Chemical Biology. Methods in Molecular Biology, vol 1263, 2015. Humana Press, New York, NY. https://doi.org/10.1007/978-1-4939-2269-7_19
33. Daina A, Michielin O, Zoete V. SwissADME: a free web tool to evaluate pharmacokinetics, drug-likeness and medicinal chemistry friendliness of small molecules. Scientific Reports- Nature, 7, 2017: 42717. doi: 10.1038/srep42717.
34. Banerjee P, Eckert AO, Schrey AK, Preissner R. ProTox-II: a webserver for the prediction of toxicity of chemicals. Nucleic Acids Research, 46(W1), 2018: W257-W263. doi: 10.1093/nar/gky318. PMID: 29718510; PMCID: PMC6031011.
35. Abraham MJ, Murtola T, Schulz R, Páll S, Smith JC, Hess B, Lindahl E. GROMACS: High performance molecular simulations through multi-level parallelism from laptops to supercomputers. SoftwareX, 1–2, 2015: 19–25.
36. Berman HM, Westbrook J, Feng Z, Gilliland G, Bhat TN, Weissig H, Shindyalov IN, Bourne PE, The Protein Data Bank. Nucleic Acids Research, 28, 2000: 235-242 https://doi.org/10.1093/nar/28.1.235.
37. Kim S, Chen J, Cheng T, Gindulyte A, He S, Li Q, Shoemaker BA, Thiessen PA, Yu B, Zaslavsky L, Zhang J, Bolton EE. Pubchem 2023 update. Nucleic Acids Research, 51 (D1), 2023: D1373-D1380. Doi: 10.1093/nar/gkac956.
38. Schüttelkopf AW, van Aalten DM. PRODRG: a tool for high-throughput crystallography of protein-ligand complexes. Acta Crystallographica Section D Biological Crystallography, 60(Pt 8), 2004:1355-63. doi: 10.1107/S0907444904011679.
39. Tian W, Chen C, Lei X, Zhao J, Liang J. CASTp 3.0: computed atlas of surface topography of proteins. Nucleic Acids Research, 46 (W1), 2018:W363-W367. doi: 10.1093/nar/gky473. PMID: 29860391; PMCID: PMC6031066.
40. The UniProt Consortium, UniProt: the Universal Protein Knowledgebase in 2023, Nucleic Acids Research, 51,(D1), 2023: D523–D531, https://doi.org/10.1093/nar/gkac1052.
41. O'Boyle NM. Towards a Universal SMILES representation-A standard method to generate

canonical SMILES based on the InChI. Journal of Cheminformatics, 4, 2012:1-4.
42. Oates PJ. Aldose reductase inhibitors and diabetic kidney disease. Current Opinion in Investigational Drugs, 11(4), 2010:402-417.
43. Kumar M, Choudhary S, Singh PK, Silakari O. Addressing selectivity issues of aldose reductase 2 inhibitors for the management of diabetic complications. Future Medicinal Chemistry, 12(14), 2020:1327-1358.
44. Kola I, Landis J. Can the pharmaceutical industry reduce attrition rates? Nature reviews Drug discovery, 3(8), 2004:711-6.
45. Kong DX, Guo MY, Xiao ZH, Chen LL, Zhang HY. Historical variation of structural novelty in a natural product library. Chemistry and Biodiversity, 8(11), 2011:1968-1977.
46. Pye CR, Bertin MJ, Lokey RS, Gerwick WH, Linington RG. Retrospective analysis of natural products provides insights for future discovery trends. Proceedings of the National Academy of Sciences, 114(22), 2017:5601-6.
47. https://www.rcsb.org/structure/1AH3. Accessed: 27 May, 2023.
48. Uddin MZ, Li X, Joo H, Tsai J, Wrischnik I, Jasti B. Rational design of peptide ligands based on knob-socket protein packing model using CD13 as a prototypereceptor, ACS Omega, 4(3), 2019:5126–5136. https://doi.org/10.1021/acsomega.8b03421.
49. Keserű GM, Makara GM. Hit discovery and hit-to-lead approaches. Drug discovery today, 11(15-16), 2006:741-8.
50. Hughes JP, Rees S, Kalindjian SB, Philpott KL. Principles of early drug discovery. British Journal of Pharmacology, 162(6), 2011:1239-1249.
51. Bowes J, Brown AJ, Hamon J, Jarolimek W, Sridhar A, Waldron G, Whitebread S. Reducing safety-related drug attrition: the use of in vitro pharmacological profiling. Nature Reviews Drug Discovery, 11(12), 2012:909-922.
52. Khan AD, Singh L. Various techniques of bioavailability enhancement: a review. Journal of Drug Delivery and Therapeutics, 6(3), 2016:34-41.
53. Lipinski CA. Lead-and drug-like compounds: the rule-of-five revolution. Drug Discovery Today: Technologies, 1(4), 2004:337-341.
54. Daina A, Michielin O, Zoete V. SwissADME: a free web tool to evaluate pharmacokinetics, drug-likeness and medicinal chemistry friendliness of small molecules. Scientific Reports, 7(1), 2017:42717.
55. Kadam RU, Roy N. Recent trends in drug-likeness prediction: a comprehensive review of in silico methods. Indian Journal of Pharmaceutical Sciences, 69(5), 2007:609.
56. Kumar M, Choudhary S, Singh PK, Silakari O. Addressing selectivity issues of aldose reductase 2 inhibitors for the management of diabetic complications. Future Medicinal Chemistry, 12(14), 2020:1327-1358.
57. Ross WE, Zwelling LA, Kohn KW. Relationship between cytotoxicity and dna strand break-age produced by adriamycin and other intercalating agents. International Journal of Radiation Oncology, Biology, Physics, 5(8), 1979:1221-4.
58. D'Aprano G, Leclerc M, Zotti G. Steric and electronic effects in methyl and methoxy substituted polyanilines. Journal of Electroanalytical Chemistry, 351(1-2), 1993:145-158.
59. Xu M, Lill MA. Induced fit docking, and the use of QM/MM methods in docking. Drug Discovery Today: Technologies, 10(3), 2013: e411-418.
60. Liu K, Watanabe E, Kokubo H. Exploring the stability of ligand binding modes to proteins by molecular dynamics simulations. Journal of Computer-Aided Molecular Design, 31, 2017:201-211.
61. Lobanov MY, Bogatyreva NS, Galzitskaya OV. Radius of gyration as an indicator of protein structure compactness. Molecular Biology, 42, 2008:623-628.